Electronic Supplementary Material (ESI) for RSC Advances.

Influence of Electronic *vs.* Steric Factors on the Solid-State Photochromic Performances of New Polyoxometalate/Spirooxazine and Spiropyran Hybrid Materials

Clotilde Menet, Hélène Serier-Brault, Olivier Oms, Anne Dolbecq, Jérôme Marrot, Ali Saad, Pierre Mialane,* Stéphane Jobic, Philippe Deniard and Rémi Dessapt*

Electronic Supplementary Information

Figure S1. Comparison of TGA measurments of (a) $SN(NO_3)$, **SN_2Mo_6** and **SN_2W_6**, and (b) $SP(NO_3)$, **SP_2Mo_6** and **SP_2W_6**

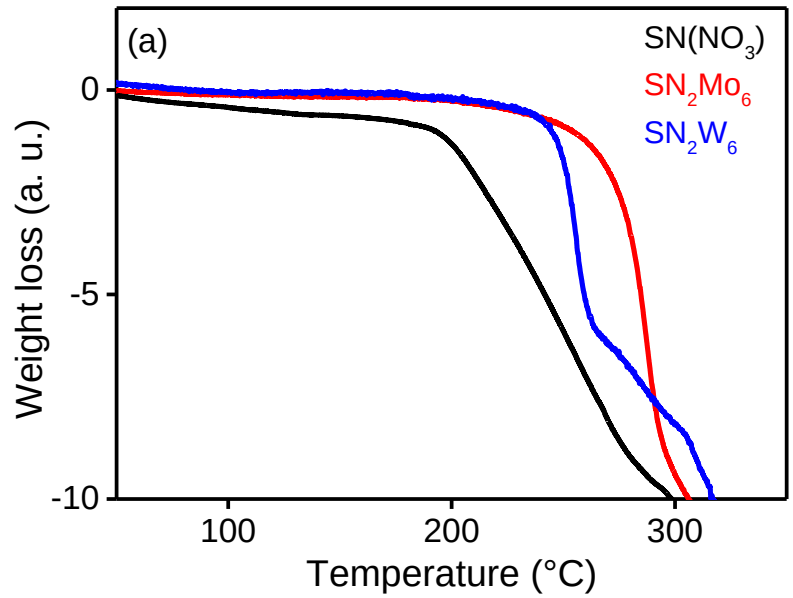

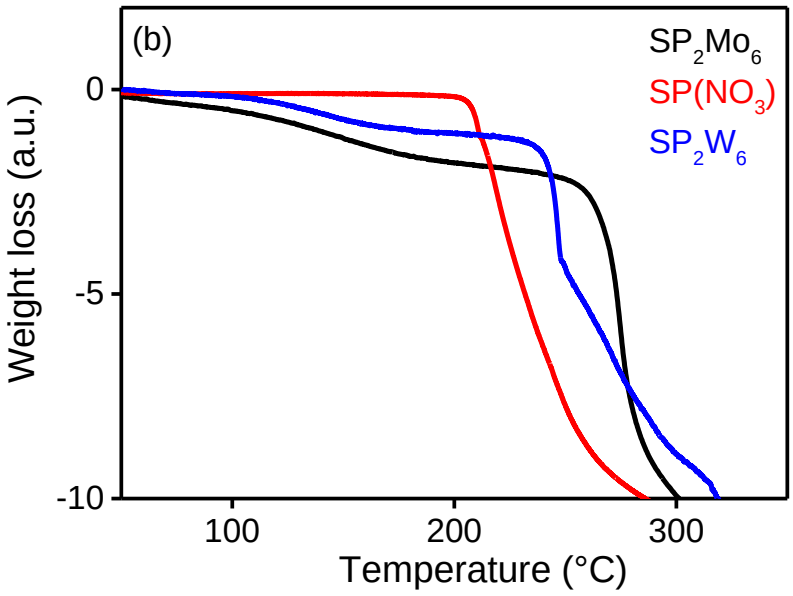

Fig. S2. Comparison of the FT-IR spectra of (a) **SN_2W_6** and (b) **SN_2Mo_6**.

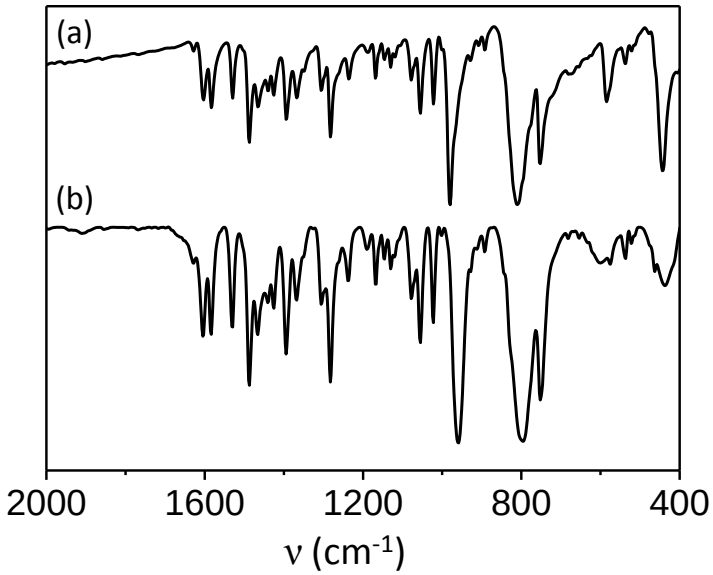

In the spectra of **SN_2W_6** and **SN_2Mo_6**, the strong absorption band in the range 1000-400 cm^{-1} are attributed to the M=O and M-O-M vibration modes of the $[M_6O_{19}]^{2-}$ anions. In addition, the spectra of **SN_2W_6** and **SN_2Mo_6** do not show any absorptions around 1670 cm^{-1}, that are characteristic of the C=O vibration of the DMF molecule.

Fig. S3. Normalized Kubelka-Munk transformed reflectivity spectra before UV irradiation of (a) **SN_2Mo_6** (black), $SN(NO_3)$ (magenta) and $(TBA)_2[Mo_6O_{19}]$ (blue), and (b) **SN_2W_6** (black), $SN(NO_3)$ (magenta) and $(TBA)_2[W_6O_{19}]$ (blue). The $\Delta\lambda$ parameter defined as $\Delta\lambda = \lambda_{max}^{(spiro)} - \lambda_{max}^{(POM)}$, with $\lambda_{max}^{(POM)}$ the low-energy LMCT transition of the POM unit. The absorption denoted by an asterisk in the spectrum of $SN(NO_3)$ is assignable to an intermolecular charge-transfer transition between SN and NO_3^- molecules due to their proximity in the crystalline state.

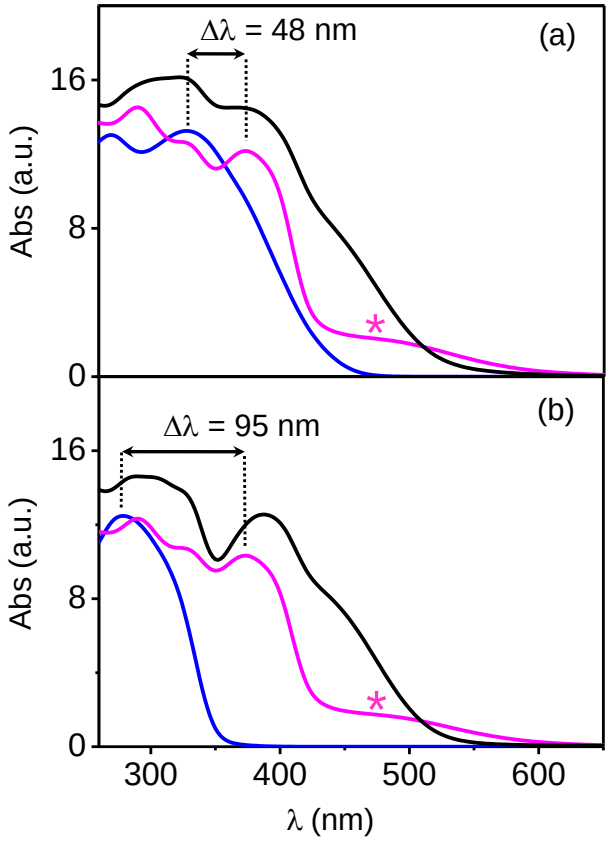

Fig. S4. UV-vis spectra in DMSO before UV irradiation of (a) **SN_2W_6** (black), $SN(NO_3)$ (red) and $(TBA)_2[W_6O_{19}]$ (blue), (b) **SN_2Mo_6** (black), $SN(NO_3)$ (red) and $(TBA)_2[Mo_6O_{19}]$ (blue), (c) **SP_2W_6** (black), $SP(NO_3)$ (red) and $(TBA)_2[W_6O_{19}]$ (blue), and (d) **SP_2Mo_6** (black), $SP(NO_3)$ (red) and $(TBA)_2[Mo_6O_{19}]$ (blue).

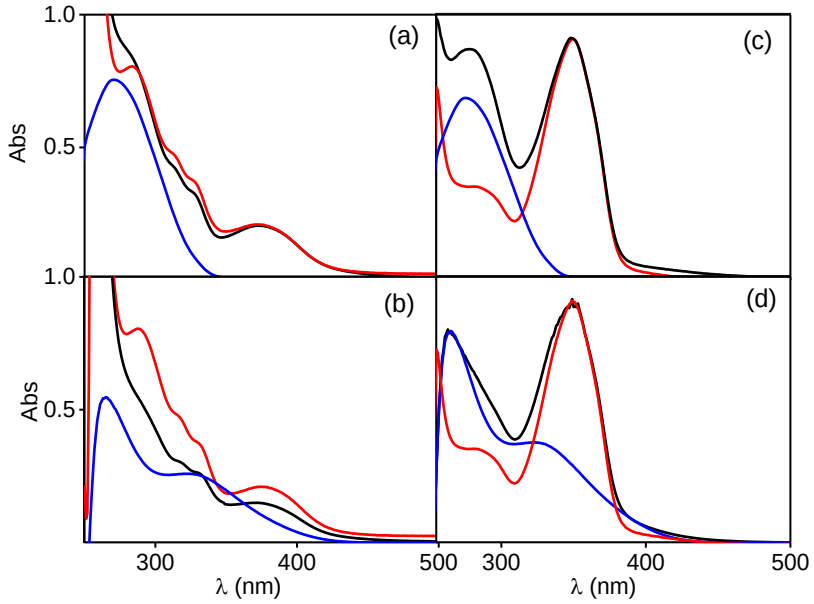

Fig. S5. Photographs of the microcrystalline powders of **SN_2W_6**, **SN_2Mo_6**, **SP_2W_6** and **SP_2Mo_6** before UV irradiation.

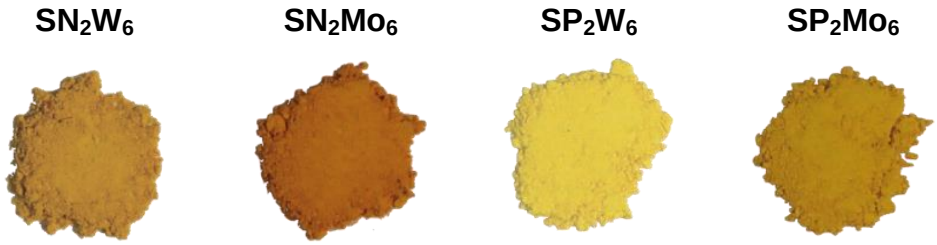

Fig. S6. Temporal evolution of the photogenerated absorption of **SN_2Mo_6** after 0, 0.166, 0.333, 0.5, 1, 2, 3, 6, 10, 15, 20 and 30 min of 365 nm-UV irradiation.

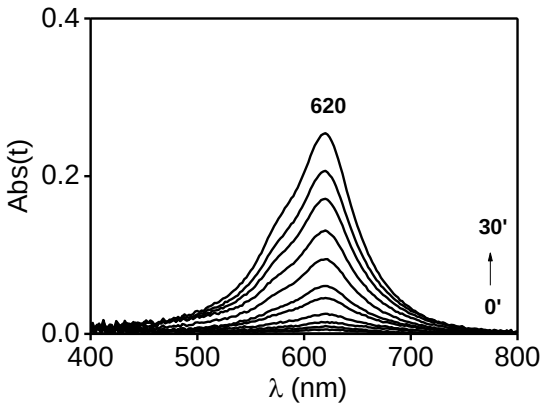

Fig. S7. (a) Comparison of the temporal evolutions at room temperature of the absorbance at 590 nm for **SP_2W_6** under orange light (λ_{ex} = 590 nm) (▲) and in the dark (●) for a sample initially irradiated for 20 min with UV light (λ_{ex} = 365 nm) (■). The dashed line shows the absorbance value just before switching off the UV light. (b) Evolution of the absorbance monitored at 590 nm for **SP_2W_6** during successive coloration/bleach cycles at room temperature. For one cycle, the sample has been exposed to UV irradiation (λ_{ex} = 365 nm) for 2 min, and then to orange light (λ_{ex} = 590 nm) for 7 min. The red line corresponds to the linear fit of $Abs^{590}(n)$ *vs n* (R^2 = 0.960).

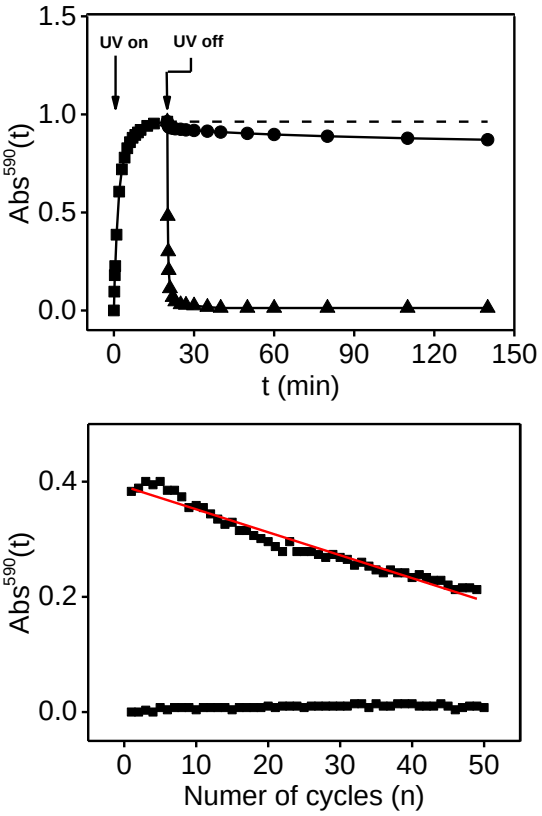

Table S1. Photocoloration kinetic parameters of **SP_2Mo_6**, **SP_2W_6**, **SN_2Mo_6** and **SN_2W_6**.

	SP_2Mo_6	**SP_2W_6**	**SN_2Mo_6**	**SN_2W_6**
$\lambda_{max}^{(MC)}$ (nm)[a]	590	590	620	620
A_1[b]	0.330	0.588	0.339	1.393
A_2[b]	0.036	0.377	0.027	0.315
$k^c_1 x10^3$ (s^{-1})[c]	0.6	13.4	0.6	10.5
$k^c_2 x10^3$ (s^{-1})[c]	9.4	3.6	12.4	125.5
R^2[d]	0.9993	0.9997	0.9998	0.9995
$t_{1/2}$ (min)[e]	15	1.3	16	0.8

[a]Photoinduced absorption band wavelength of the merocyanin form of the spiro-molecule. [b]The $Abs^{\lambda max}(t)$ *vs t* plots were fitted as $Abs^{\lambda max}(t) = -A_1-A_2 + A_1\exp(-k^c_1 t) + A_2\exp(-k^c_2 t)$. [c]Coloration rate constants. [d]Regression coefficient for the $Abs^{\lambda max}(t)$ *vs t* plots. [e]coloration half-life time.

Table S2. Fading kinetic parameters of **SN_2W_6** and **SP_2W_6**.

Fading under yellow light

	SN_2W_6	**SP_2W_6**
λ_{max}[a] (nm)	620	590
A_0	1.691	0.850
A_1[b]	0.972	0.699
A_2[b]	0.66	0.135
$k^c_1 \times 10^3$ (s^{-1})[c]	48.8	71.3
$k^c_2 \times 10^3$ (s^{-1})[c]	3.3	7.7
R^2[d]	0.9960	0.9997

Thermal fading

	SN_2W_6	**SP_2W_6**
λ_{max}[a] (nm)	620	590
A_0	1.717	0.863
A_1[b]	0.027	0.033
A_2[b]	0.070	0.066
$k^c_1 \times 10^3$ (s^{-1})[c]	33.9	44.0
$k^c_2 \times 10^3$ (s^{-1})[c]	0.3	0.3
R^2[d]	0.9970	0.9981

[a]Photoinduced absorption band wavelength. [b]The $Abs^{\lambda max}(t)$ *vs t* plots were fitted as $Abs^{\lambda max}(t) = (A_0-A_1-A_2) + A_1\exp(-k^f_1 t) + A_2\exp(-k^f_2 t)$. [c]Coloration rate constants. [d]Regression coefficient for the $Abs^{\lambda max}(t)$ *vs t* plots.